

Indanylacetic acid derivatives carrying aryl-pyridyl and aryl-pyrimidinyl tail groups—new classes of PPAR γ/δ and PPAR $\alpha/\gamma/\delta$ agonists

Louis-David Cantin,^{a,*} Sidney Liang,^a Herbert Ogutu,^a Christiana I. Iwuagwu,^a Ken Boakye,^c William H. Bullock,^a Michael Burns,^c Roger Clark,^a Thomas Claus,^c Fernando E. delaCruz,^c Michelle Daly,^c Frederick J. Ehrigott,^a Jeffrey S. Johnson,^a Christine Keiper,^c James N. Livingston,^c Robert W. Schoenleber,^a Jeffrey Shapiro,^c Christopher Town,^b Ling Yang,^c Manami Tsutsumi^c and Xin Ma^a

^aDepartment of Chemistry Research, Bayer Pharmaceuticals Corporation, West Haven, CT 06516, USA

^bDepartment of Research Technologies, Bayer Pharmaceuticals Corporation, West Haven, CT 06516, USA

^cDepartment of Metabolic Disorders Research, Bayer Pharmaceuticals Corporation, West Haven, CT 06516, USA

Received 20 October 2006; revised 7 November 2006; accepted 8 November 2006

Available online 15 November 2006

Abstract—Modulation of PPAR activities represents an attractive approach for the treatment of diabetes with associated cardiovascular complications. The indanylacetic acid structural motif has proven useful in the generation of potent and tunable PPAR ligands. Modification of the substituents on the linker and the heterocycle tail group allowed for the modulation of the selectivity at the different receptor subtypes. Compound **33** was evaluated in vivo, where it displayed the desired reduction of glucose levels and increase in HDL levels in various animal models.

© 2006 Elsevier Ltd. All rights reserved.

Diabetes, together with its complications, was responsible for 1 in 5 deaths in the US in 2002.¹ The World Health Organization is now forecasting that by the year 2030, 366 million people will suffer from diabetes worldwide,² with 90% of these cases due to non-insulin-dependent (or Type II) diabetes.¹ As the disease progresses, numerous complications gradually erode the quality of life of patients. The greater prevalence of cardiovascular complications² in diabetics underscores the need to develop antidiabetic agents capable of lowering HbA1c levels while improving the lipid profile of patients. Such multi-action agents may hold promise for delaying the progression of the disease, as suggested by the increasing evidence identifying obesity as a cause factor of Type II diabetes and concomitant cardiovascular complications.

Correction of the elevated glucose levels in patients with Type II diabetes is typically achieved through modulation of insulin production, of glucose neogenesis, or by improving glucose uptake by muscle tissues in response to insulin.³ The gradual increase in skeletal muscle tissue resistance to insulin has also been linked to a cascade of events leading to Type II diabetes and eventually to β -cell failure. Physicians have attempted to slow the progression of insulin resistance by the use of insulin sensitizers such as PPAR (peroxisome proliferator-activated receptor) gamma agonists. This class of agents, typified by the glitazones, has received significant attention from the pharmaceutical industry leading to the successful development of two agents, rosiglitazone and pioglitazone, currently used for the management of elevated glucose levels.⁴ The sustained research interest in these agents is due to the various roles that PPARs can play in controlling glucose homeostasis, as well as triglyceride (TG) and cholesterol levels.⁵ Indeed, PPAR α agonists, such as fibrates, have played a long-standing role in modulation of triglyceride levels,⁶ and there is now increasing evidence that PPAR δ agonists can improve

Keywords: PPAR agonist; Indanyl acetic acid; Diabetes; Cardiovascular; Triglycerides; HDL; Cholesterol; SAR.

* Corresponding author. Tel.: +1 203 812 3968; e-mail: david.cantin.b@bayer.com

high-density lipoprotein (HDL)/low-density lipoprotein (LDL) profiles in animals.⁷

A previous report from our laboratories disclosed PPAR α/γ agonists incorporating a novel indanylacetic acid head-group.⁸ This work led to the identification of compounds capable of correcting glucose levels, as well as modulating TG levels. Herein, we report on further modifications to indanylacetic acid, which lead to PPAR agonists that incorporate PPAR δ activity.

Starting from our first generation agonists (**1**, Fig. 1), we hypothesized that linking an unsubstituted indanylacetic acid with six-membered heteroaryl group using a flexible linker could provide us with a dual or triple agonist (**2**, Fig. 1).

The synthesis of the indane fragment (Scheme 1) started from indanone **3** which was converted to the corresponding enoate under Reformatsky-type conditions.⁹ Subsequent reduction and hydrolysis provided acid **4**, which underwent chemical resolution using (*S*)-(-)- α -methylbenzylamine to provide **5** in good yield and high enantiomeric excess. With **5** in hand, esterification of **5** followed by demethylation provided the right-hand fragment **6** of the target compounds.

The synthesis of the left-hand moiety of the target compounds was achieved starting from an appropriately substituted 2,4-dichloropyridine (**7**) onto which the amino alcohol linker was introduced chemoselectively at the C4 position using sodium carbonate in ethanol (Scheme 2). Subsequent etherification using a modified Mitsunobu protocol allowed for the introduction of the indane **6** in good yield, followed by treatment with NaH and methyl iodide to provide the key intermediate **8**. Finally, Suzuki cross-coupling, followed by saponification, provided compound **9**.

We began our optimization work by exploring the SAR at the C2 position of the pyrimidine. The task of optimizing for all three activities was simplified since most variations at C2 led to potent PPAR δ ligands (Table 1). With our attention focused on improving PPAR α and PPAR γ potencies, we began by introducing lipophilic groups at the *para*-position of the C2 phenyl ring (11–14, Table 2), which provided increased potency at PPAR γ and PPAR α . Introduction of both electron-do-

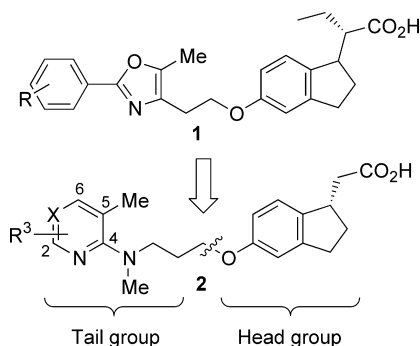
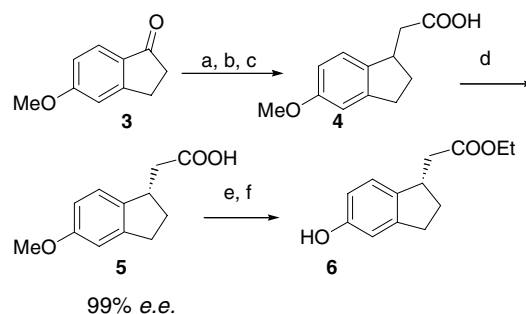
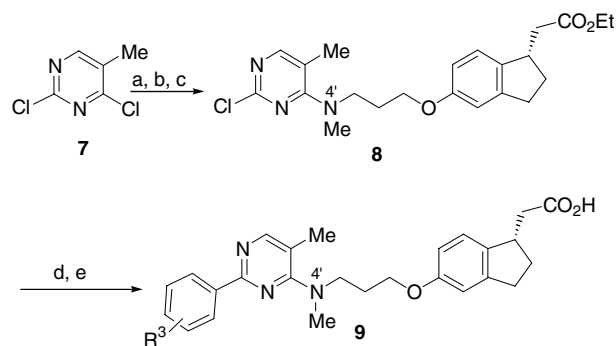


Figure 1.



Scheme 1. Reagents and conditions: (a) Zn, ethyl bromoacetate, THF, 40 °C; (b) H₂ (40 psi), 5% Pd/C, EtOH, 99% yield (two steps); (c) NaOH, H₂O, EtOH, reflux, 80% yield; (d) (*S*)-(-)- α -methylbenzylamine, acetone; recrystallization; 1 N HCl, EtOAc, 35% yield, 99% ee; (e) TMSCl, EtOH, 98% yield; (f) AlCl₃, EtSH, CH₂Cl₂, 5–10 °C, 96% yield.

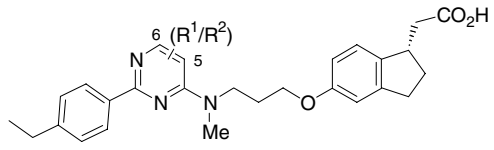


Scheme 2. Reagents and conditions: (a) 1,3-propanolamine, NaHCO₃, EtOH, 95% yield; (b) **6**, ADDP, PPh₃, THF, 95% yield; (c) NaH, MeI, DMF, 60% yield; (d) Ar-B(OH)₂, PdCl₂(dppf)-CH₂Cl₂, Na₂CO₃, H₂O, 1,4-dioxane, toluene; (e) LiOH, H₂O, THF, EtOH, 40–60% yield (two steps).

Table 1.

Compound	R ³	IRBA ¹⁰ (EC ₅₀ , nM)	PPAR δ ¹¹	
			FRET (EC ₅₀ , nM)	FRET (EC ₅₀ , nM)
10	H	678	6610	24
11	4-Me	780	1150	9
12	4-Et	145	200	10
13	4- <i>i</i> Pr	29	990	34
14	4- <i>t</i> -Bu	156	641	28
15	4-EtO	161	3090	58
16	4-MeO	7010	1390	12
17	4-Ac	237	6550	83
18	4-F	860	2120	7
19	4-Cl	2800	1130	7
20	3-Me	670	4390	41
21	3-EtO	6930	3540	7
22	3-Cl	582	2370	23

Table 2.



Compound	R ¹ /R ²	IRBA ¹⁰ (EC ₅₀ , nM)	PPAR α ¹¹ FRET (EC ₅₀ , nM)	PPAR δ ¹¹ FRET (EC ₅₀ , nM)
23	H	800	565	25
24	5-F	360	425	16
12	5-Me	145	200	10
25	5-Et	950	120	2
26	6-Me	600	920	11

nating (**15** and **16**) and withdrawing groups (**17–19**) tended to decrease the PPAR α potency relative to lipophilic substituents. Migration of the substituent to the *meta*-position of the phenyl ring caused a loss in potency at PPAR α and PPAR δ as exemplified by compounds **20** and **22**. In contrast, a 3-EtO group (**21**) caused a significant increase in potency at PPAR δ over the corresponding 4-EtO (**15**), while the PPAR α potency remained unaffected. These group migrations caused different effects on PPAR γ potency where the 3-EtO (**21**) showed decreased potency and the 3-Cl (**22**) provided a moderate (4- to 5-fold) increase in potency vs its 4-Cl analog (**19**). Further substitution at the *ortho*-position, or introduction of two substituents (2,4 or 3,4), led to compounds with decreased potency at one or more receptor subtypes.

Turning our attention to the effects of the substituents on the pyrimidine ring, it rapidly became apparent that the size and location of the substituent was critical for retaining the activity (Table 2). Indeed, while the 5-methyl group (**12**) was optimal, the 5-ethyl and 6-methyl groups (**25** and **26**) decreased potency at either PPAR α or PPAR γ . In addition, introduction of a fluorine atom at position 5 (**24**) was tolerated by all three receptor subtypes.

Having completed the initial optimization, several compounds were selected for further pharmacological profiling. Cell assays¹² performed on compound **12** confirmed its potent agonist activity at PPAR α and δ ¹³ with a 10-fold decrease in potency from the human receptor to the mouse receptor. Surprisingly, compound **13** proved to be more potent than expected as a PPAR α agonist in CV-1 cells, while maintaining the same species preference for the human receptor.¹³

Having identified compounds with the targeted activity profile, we evaluated the pharmacokinetic profile of several analogs. An initial screen using rodent and human microsomes revealed that the compounds were rapidly metabolized. Subsequent in vivo experiments confirmed an overall trend toward low plasma exposure when either compound **12** or **13** was dosed orally in rodents (mice and rats). Although establishing a direct correlation between microsomal stability and oral exposure is

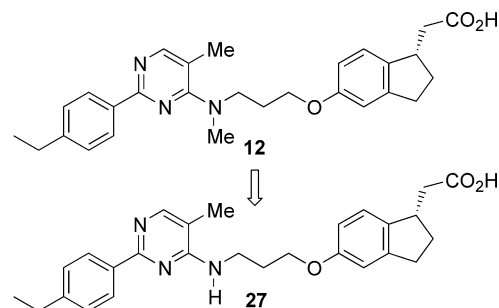
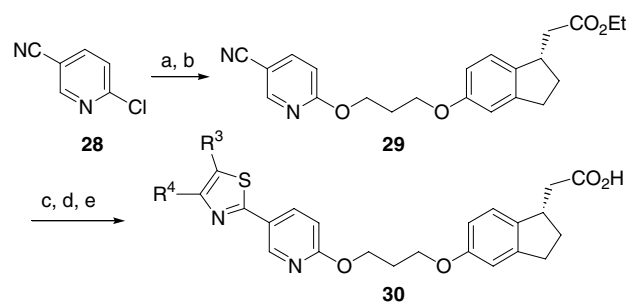


Figure 2.

often difficult, we sought nonetheless to identify the major metabolites to help guide our optimization work. We suspected that the *N*-methyl group might be the origin of this instability (Fig. 2), which was confirmed by in vitro metabolite identification studies. Although we observed other less prevalent metabolites, the *N*-demethylated products were consistently the major metabolites observed.

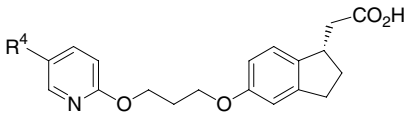
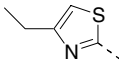
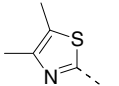
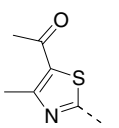
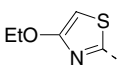
Compound **27** was found to be a weak ligand for all receptors except PPAR δ (56 nM). Modifications of the linker in an attempt to block metabolism revealed that this area of the molecule was critical for maintaining the potency at all three receptor subtypes. Indeed, introduction of sterically hindered groups or cyclization led to a decrease in potency (data not shown). However, exchanging the *N*-Me group for an oxygen atom to remove the site of metabolism was better tolerated (IRBA: 1600 nM, PPAR α FRET: 900 nM, PPAR δ FRET: 5 nM). The activity profile of the ether-linked agonists was optimized by incorporating our findings with those of a related project,¹⁴ where a phenyl ring bearing a thiazole in the *para*-position to the linker was beneficial.

Using the 2,4-substituted pyrimidines did not offer the opportunity to introduce a substituent in the *para*-position to the linker. Additionally, we had previously determined that the other pyrimidine isomers were less favored. We therefore opted to change the heterocycle to a pyridine, which allowed for the desired substituent orientation and was expected to provide similar physicochemical properties to the pyrimidines.



Scheme 3. Reagents and conditions: (a) 1,3-propanediol, NaH, DMF, 83% yield; (b) **6**, ADDP, PPh₃, THF, 67% yield; (c) H₂S, Et₃NH, DMF, 86% yield; (d) 2-haloketones, EtOH, 70 °C; (e) LiOH, H₂O, THF, EtOH, 60–80% yield (two steps).

Table 3.

				
Compound	R ⁴	IRBA ¹⁰ (EC ₅₀ , nM)	PPAR α ¹¹ FRET (EC ₅₀ , nM)	PPAR δ ¹¹ FRET (EC ₅₀ , nM)
31		264	421	3
32		511	6780	5
33		35	1390	9
34		411	807	3

A series of O-linked pyridines bearing a thiazole substituent were synthesized as described in Scheme 3. Addition of 1,3-propane diol to 5-chloronicotinonitrile (**28**), followed by Mitsunobu etherification with indane **6**, provided intermediate **29**. Conversion of the nitrile group to the corresponding thioamide was achieved by exposure to H₂S in DMF at 40 °C. Subsequent Hantzsch-type condensation of diversely substituted halo ketones, followed by basic hydrolysis, provided the target compound **30**.

A series of thiazoles were prepared, from which compound **33** emerged as a compound of potential interest (Table 3). Although the potency at PPAR α was weaker than anticipated, the potent PPAR γ and δ activities prompted us to further profile this compound. The activity profile translated well to human cell assays,¹⁵ however compound **33** showed a significant decrease in potency (>20-fold) in mouse PPAR δ cell assay (human PPAR δ in CV-1 cells (IC₅₀) 56 nM; mouse PPAR δ in CV-1 cells (IC₅₀) 1390 nM).

Pleasingly, compound **33** provided the desired improvement in pharmacokinetic profile in rodents [e.g., rats (PO and IV, 3 mpk) PO AUC 26 μ M h, C_{max} 2.8 μ M; *F* 48%, *t*_{1/2} = 5 h]. This improved exposure profile, which was found to be similar in mice, allowed us to evaluate compound **33** in diabetic animal models. Compound **33** reduced plasma glucose levels in *db/db* mice in a dose-dependent manner with an estimated ED₅₀ value of 6.7 mpk after 7 days of dosing (Fig. 3).¹⁶ At a dose of 10 mpk, compound **33** proved to be as efficacious in lowering glucose as the maximally effective dose of rosiglitazone in this model (not shown). Similarly, when administered for 10 days at a dose of 10 mpk, compound **33** normalized glucose tolerance in Zucker *fafa* rats (Fig. 4).¹⁶

The ability of compound **33** to modulate TG and HDL-cholesterol levels through its effects on PPAR δ was

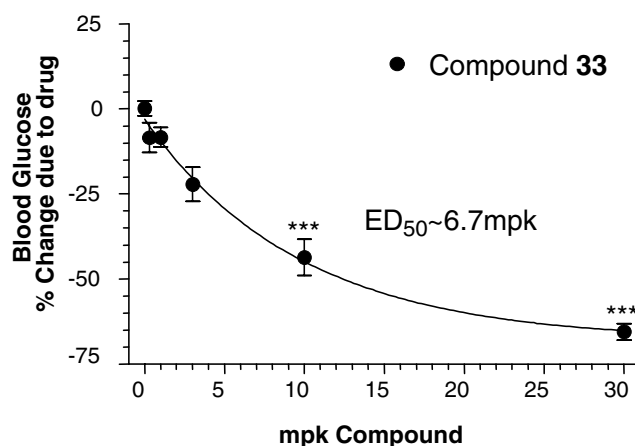


Figure 3. Effects of **33** on blood glucose levels in *db/db* mice after 7 days of treatment.

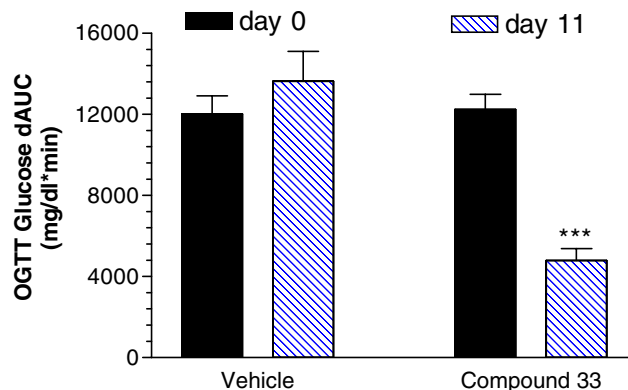


Figure 4. Effects of **33** on glucose tolerance in Zucker *fa/fa* rats after 10 days of treatment.

assessed using hApoA1 mice. Oral administration of **33** to hApoA1 mice at 30 mpk (to account for the weaker cell potency at murine PPAR δ) for 10 days¹⁶ reduced

plasma triglycerides [$-32 \pm 7\%$ ($p < 0.05$)] and raised HDL-cholesterol [$22 \pm 7\%$ ($p < 0.05$)].

In summary, we have shown that the indanylacetic acid group is a versatile head-group, which can be combined to diverse tail groups to generate PPAR agonists with different receptor subtype selectivity. The optimization of the tail group allowed for the identification of both PPAR γ/δ dual and PPAR $\alpha/\gamma/\delta$ triple agonists. The anti-diabetic properties of this scaffold were demonstrated, together with added benefits of correcting TG and HDL levels associated with agonism of PPAR δ .¹⁷

Acknowledgments

We thank Jefferson Chin, László Musza, and Anthony Paiva for NMR and LC-MS support. We are also grateful to Drs. Roger A. Smith and Derek Lowe for helpful discussions.

References and notes

1. Stumvoll, M.; Goldstain, B. J.; van Haeften, T. W. *The Lancet* **2005**, *365*, 1333.
2. Zimmet, P.; Alberti, K. G.; Shaw, J. *Nature* **2001**, *414*, 782.
3. Krentz, A. J.; Bailey, C. J. *Drugs* **2005**, *66*, 385.
4. Campbell, I. W. *Curr. Mol. Med.* **2005**, *5*, 349.
5. For leading references, see: (a) Staels, B.; Fruchart, J.-C. *Diabetes* **2005**, *54*, 2460; (b) Cheng, P. T. W.; Mukherjee, R. *PPARs as targets for metabolic and cardiovascular diseases* **2005**, *5*, 741.
6. Robillard, R.; Fontaine, C.; Chinetti, G.; Fruchart, J.-C.; Fibrates Staels, B. *Handb. Exp. Pharmacol.* **2005**, *170*, 389.
7. Oliver, W. R.; Shenk, J. L.; Snaith, M. R.; Russell, C. S.; Plunket, K. D.; Bodkin, N. L.; Lewis, M. C.; Winegar, D. A.; Sznajdman, M. L.; Lambert, M. H.; Xu, H. E.; Sternbach, D. D.; Klier, S. A.; Hansen, B. C.; Willson, T. M. *Proc. Natl. Acad. Sci. U.S.A.* **2001**, *98*, 5306.
8. Lowe, D. B.; Bifulco, N.; Bullock, W. H.; Claus, T.; Coish, P.; Dai, M.; Dela Cruz, F. E.; Dickson, D.; Fan, D.; Hoover-Litty, H.; Li, T.; Ma, X.; Mannelly, G.; Monahan, M.-K.; Muegge, I.; O'Connor, S.; Rodriguez, M.; Shelekhn, T.; Stolle, A.; Sweet, L.; Wang, M.; Wang, Y.; Zhang, C.; Zhang, H.-J.; Zhang, M.; Zhao, K.; Zhao, Q.; Zhu, J.; Zhu, L.; Tsutsumi, M. *Bioorg. Med. Chem. Lett.* **2006**, *16*, 297.
9. All compounds described gave consistent ¹H NMR and LC/MS data. For more details on their synthetic preparations, see: Cantin, Louis-David; Choi, Soongyu; Clark, Roger B.; Hentemann, Martin F.; Ma, Xin; Rudolph, Joachim; Liang, Sidney X.; Akuche, Christiana; Lavoie, Rico C.; Chen, Libing; Majumdar, Dyuti; Wickens, Philip L. Preparation of indaneacetic acid derivatives and their use as pharmaceutical agents, WO 2004058174.
10. The PPAR γ activity was assessed by IRBA, a cell-based assay performed in mouse 3T3-L1 pre-adipocytes. This assay measures the ability of a test compound to cause an increase in the number of insulin receptors and hence is an index of the insulin sensitizing activity. 3T3-L1 cells were seeded in 96-well tissue culture plates using DMEM containing 10% fetal bovine serum, 1% pen/strep, and 2 mM L-glutamine, and were grown until they were 2 days post-confluent. Cells were then treated for 2 days with medium containing 0.5 μ M human IGF-1 and test compound. After treatment, the medium was replaced with medium free of IGF-1 and compound, and incubated for 4 days. After washing the cells with buffer, they were incubated with 0.1 nM ¹²⁵I-insulin and (\pm) 100 nM unlabeled insulin, and incubated at rt for 1 h. The cells were then washed 3 \times with buffer, dissolved with 1 N NaOH, and the amount of radioligand bound was measured using a gamma counter. Values reported are means of at least two experiments.
11. PPAR α and PPAR δ activity was measured using a fluorescence resonance energy transfer (FRET) assay using the human PPAR α and PPAR δ ligand-binding domains. Test compounds were incubated in 96-well plates with europium-labeled anti-GST antibody, GST-tagged PPAR ligand-binding domain, biotinylated REB-binding protein, and streptavidin-labeled APC (Wallac, AD0065). The plate was read in a fluorimeter with an excitation wavelength of 340 nm and emission wavelengths of 615 and 640 nm. Values reported are means of at least two experiments.
12. PPAR α and PPAR δ activity was measured using a cell-based GAL4 transactivation assay for human and mouse ligand-binding domain in CV-1 cells. CV-1 cells were seeded in 96-well plates at 2.8×10^4 cells per well, grown overnight in standard media containing 10% fetal bovine serum, and then transiently transfected using the Lipofectamine/Plus procedure. The cells in each well were transfected with plasmids containing the Gal4/PPAR-LBD fusion, UAS/firefly luciferase, and *Renilla* luciferase. After an overnight incubation with media containing 10% FBS treated with charcoal/dextran, test compounds were added and the cells were incubated for an additional 24 h. The plates were processed using the Promega Dual Luciferase kit and read on a Packard Topcount. EC₅₀ values were determined based on a dose-response curve and the percent maximum stimulation was assessed by comparison to reference compounds. Values reported are means of at least two experiments.
13. Compound **12**: human PPAR δ CV-1 cells IC₅₀ 30 nM; human PPAR α CV-1 cells IC₅₀ 175 nM; mouse PPAR δ CV-1 cells IC₅₀ 370 nM; mouse PPAR α CV-1 cells IC₅₀ 670 nM. Compound **13**: human PPAR δ CV-1 cells IC₅₀ 49 nM; human PPAR α CV-1 cells IC₅₀ 237 nM; mouse PPAR δ CV-1 cells IC₅₀ 610 nM; mouse PPAR α CV-1 cells IC₅₀ 2530 nM.
14. Rudolph, J.; Chen, L.; Majumdar, D.; Bullock, W.H.; Burns, M.; Choi, S.; Claus, T.; Dela Cruz, F.E.; Daly, M.; Ehrgott, F.J.; Johnson, J.S.; Livingston, J.N.; Nophsker, M.; Schoenleber, R.W.; Shapiro, J.; Tomlinson, S.; Town, C.; Yang, L.; Tsutsumi, M.; Ma, X. *Abstracts of Papers*, 232nd ACS National Meeting, Sept 10–14, 2006; MEDI-377.
15. Compound **33**: human PPAR δ CV-1 cells IC₅₀ 56 nM; human PPAR α CV-1 cells IC₅₀ > 6000 nM; mouse PPAR δ CV-1 cells IC₅₀ 1390 nM.
16. *In vivo studies (mice and rats)*. All animals were purchased at 6 weeks of age and were maintained on standard laboratory rodent chow ad libitum. *db/db* and *hApoA1* Mice experiments. Female *db/db* mice and male *hApoA1* mice were purchased from The Jackson Laboratory (Bar Harbor, ME). The *hApoA1* mice were used within 2 weeks of their arrival, whereas the *db/db* mice were maintained on diet for 3–4 weeks and 8–10 weeks, respectively, prior to starting the study. The average body weight was 25 g for the *db/db* mice and 50 g for the *hApoA1* mice. The animals were weighed and tail-bled prior to the start of study. Plasma from *db/db* mice was analyzed for glucose levels using either a Beckman Glucose Analyzer 2

(Beckman Instruments, Fullerton, CA) or a Technicon Axon autoanalyzer (Bayer HealthCare LLC, Tarrytown, NY). Plasma from hApoA1 mice was analyzed for triglyceride and HDL-cholesterol levels using the Axon autoanalyzer. The animals were arranged into the appropriate number of groups with each group having the same mean plasma glucose levels (*db/db* mice) or plasma triglyceride levels (hApoA1 mice) prior to dosing. All animals then were orally dosed once daily with vehicle (0.5% methylcellulose in water), a positive control compound, or compound **33**. The *db/db* and hApoA1 mice were dosed for 7 days. All animals were fed ad libitum throughout the study. Approximately 24 h after the last dose, the animals were weighed and bled again and the plasma analyzed for glucose, triglycerides or HDL-cholesterol. *Calculation of percent change due to drug treatment.* In order to evaluate the effects of compound **33** treatment on glucose levels and on triglyceride and HDLc levels, it is useful to calculate the percent change in glucose or triglyceride and HDLc that is due to drug treatment. This takes into account any changes that may have occurred in the vehicle-treated animals during the study. The percent change due to drug treatment is calculated as follows: $\left(\frac{T_f/T_i}{V_f/V_i} - 1\right) * 100$ T_f and T_i are the final and initial values of either plasma glucose or serum triglyceride levels in the drug-treated animals, respectively, and V_f and V_i are the same for the vehicle-treated animals. A positive number denotes a drug-induced increase, whereas a negative number denotes a drug-induced decrease. *fal/fa rat glucose*

tolerance experiments. Female Zucker Fatty (*fal/fa*) rats were purchased from Charles River (Wilmington, MA). Animals were maintained on diet for 8–10 weeks, prior to starting the study. The average body weight was 471 g. Female *fal/fa* rats were fasted overnight and given a 2 g/kg IPGTT. Blood glucose was measured from tail to tip blood using a Glucometer (Bayer HealthCare LLC, Mishawaka, IN) just prior to the glucose load and after 15, 30, 60, 90, and 120 min. The glucose area-under-the-curve (AUC) was calculated over the 0-to-120 min using the trapezoidal method, and the rats were grouped with equivalent mean glucose AUC values. Starting a week later, the rats were dosed daily with vehicle (0.5% methylcellulose) or 10 mg/kg compound **33** for 10 days. The rats were fasted overnight and a 2 g/kg IPGTT performed again on day 11. *Statistical analysis.* All results are expressed as the means \pm SEM for the number of animals indicated in the figure legends. ANOVA was used to evaluate the effects of positive control drugs and compound **33** using InStat (GraphPad Software Inc., San Diego, CA). The Tukey–Kramer multiple comparisons test was used for the parametric ANOVA. Whenever a non-parametric ANOVA was required, the Kruskal–Wallis test was used. Results were considered significant at $p < 0.05$.

17. Xu, Y.; Etgen, G. J.; Broderick, C. L.; Canada, E.; Gonzalez, I.; Lamar, J.; Montrose-Rafizadeh, C.; Oldham, B. A.; Osborne, J. J.; Xie, C.; Shi, Q.; Wimmeroski, L. L.; York, J.; Yumibe, N.; Zink, R.; Mantlo, N. *J. Med. Chem.* **2006**, *49*, 5649.